ELSEVIER

Journal of Magnetism and Magnetic Materials 217 (2000) 19–26

Journal of magnetism and magnetic materials

www.elsevier.com/locate/jmmm

Jahn–Teller domains and magnetic domains in Mn_2FeO_4

J. Kub[a,*], V. Brabers[b], P. Novák[a], R. Gemperle[a], J. Šimšová[a]

[a]*Institute of Physics AS CR, Na Slovance 2, 182 21 Prague 8, Czech Republic*
[b]*Department of Physics, Eindhoven University of Technology, Eindhoven, The Netherlands*

Received 24 January 2000; received in revised form 14 March 2000

Abstract

Elastic (Jahn–Teller) domains and magnetic domains in the tetragonal spinel Mn_2FeO_4 were studied using X-ray double-crystal topography, X-ray diffractometry and the colloid-SEM method. The Jahn–Teller domains of the measured samples are tetragonal with the [0 0 1] *c*-axis alternating perpendicularly (thick domains) and parallel (thin domains) with respect to the growth direction of the specimens. Boundary interfaces are of the (1 1 0) type consistent with the cubic spinel system. A complex magnetic domain structure is discussed in relation with the crystallographic orientation of the Jahn–Teller domains.

PACS: 75.60

Keywords: Ferrites; Ferroelastic domains; Magnetic domains

1. Introduction

The tetragonal structure of Mn_2FeO_4 originates from a co-operative Jahn–Teller effect [1] associated with the alignment of the Mn^{3+} ions occupying tetragonally distorted octahedra formed by the oxygen ions in the spinel lattice. Formerly, the Jahn–Teller domains – 'dagger-shaped' domains limited by (1 1 0) planes were observed by electron microscopy [1]. The aim of this paper is to study the Jahn–Teller domains of the bulk tetragonal Mn_2FeO_4 in more detail using X-ray double-crystal topography and X-ray diffractometry [2]. As the Jahn–Teller domain size decreases with decreasing thickness of the sample we can expect larger Jahn–Teller domains in our samples as compared with the results made on very thin slices reported in Ref. [1].

Additionally, in the present paper the magnetic domain structure is visualised by the colloid-SEM method [3] on two different planes of tetragonal Mn_2FeO_4 and correlated with the Jahn–Teller crystallographic domain structure. Moreover, the hysteresis loop measurements were performed by vibrating sample magnetometer (VSM), to relate the bulk magnetisation with the surface magnetic domain structure.

2. Samples

Lamellar samples of tetragonal spinels Mn_2FeO_4 were grown in air by a zone melting process of polycrystalline bars [4]. As seed crystal a

* Corresponding author. Fax: + 420-2-821227.
E-mail address: kub@fzu.cz (J. Kub).

0304-8853/00/$ - see front matter
PII: S0304-8853(00)00335-8

[1 0 0]-oriented cubic spinel crystal with the composition of $Mn_{1.9}Fe_{2.1}O_4$ was used. At room temperature Mn_2FeO_4 has a tetragonally distorted spinel structure, but at 200°C a first-order transition occurs, due to the thermal misalignment of the tetragonally deformed $Mn^{+3}O_6^{2-}$ octahedra [1] stabilising the high-temperature cubic spinel structure.

The recrystallised Mn_2FeO_4 bars grow epitaxially on the seed crystal with the [1 0 0] axis along the growth direction. Upon cooling to room temperature, the cubic crystals transform into lamellar specimens because of a reorientation of the tetragonal *c*-axis at the cubic–tetragonal transition in three perpendicular directions, one of them being the growth direction of the recrystallised bar. By using the annealing process described in Ref. [5], an alignment of the *c*-axis of these specimens could be achieved, resulting in a more coarse-grained texture.

The room-temperature lattice parameters for the spinel structure were determined on a powdered sample by X-ray diffraction; $a = 8.3722$ Å and $c = 8.8521$ Å. No X-ray line broadening, indicative of a Mn^{3+} clustering, i.e., the onset of a phase segregation into a cubic and a tetragonal spinel, was observed, which implies that the specimens are homogeneous in composition. For our experiment two rectangular samples were cut from annealed specimens: sample No. 1 – an unpolished prism of $5 \times 5 \times 20$ mm and sample No. 2 – a polished cube with dimension $4 \times 4 \times 4$ mm.

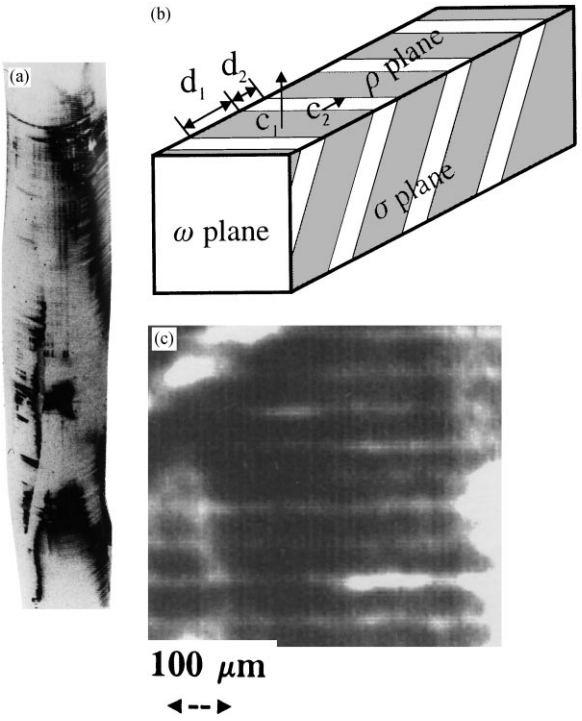

Fig. 1. (a) Double-crystal topography of sample No. 1 (plane ρ) - full view. The distinct U-shape patterns represent growth striations, while the thin parallel stripes perpendicular to the long axes of the sample (i.e. to the growth direction) are the image of Jahn–Teller domains. (b) Schematic presentation of the crystallographic orientation of Jahn–Teller domains. (c) Image of Jahn–Teller domains - details of Fig. 1a with larger magnification.

3. Jahn–Teller domains

The Jahn–Teller 'lattice' domains were studied by the X-ray double-crystal topography in (Si 2 2 0, $-$ Mn_2FeO_4 4 0 0) nearly parallel setting. The full topograph of sample 1 is shown in Fig. 1a. The sample consists of several large grains which are only slightly mutually misoriented ($\sim 0.05°$). The distinct U-shaped patterns correspond to the growth striations, whereas parallel patterns are caused by the Jahn–Teller domains. A schematic representation of the crystal and the observed Jahn–Teller domain structure is given in Fig. 1b. On the rectangular sample three planes are distinguished: the ω plane, which is perpendicular to the growth direction, originally the cubic [1 0 0] direction and the ρ and σ planes which are parallel to the growth direction and which coincide with the high-temperature cubic (0 1 0) and (0 0 1) spinel planes, respectively. The whole domain area consists of alternating thin and thick domains, which can clearly be seen in detail on an enlarged part of the crystal (Fig. 1c). The boundaries between these domains coincide with the (1 1 0) planes of the spinel structure [1].

The tetragonal deformation of the diffracting (i.e., dark) thicker domains with thickness d_1 is perpendicular to the plane ρ of the sample, i.e. $c_1 \sim$ [0 0 1] direction (see Fig. 1b). In the thinner domains (thickness d_2) the tetragonal c_2-axis is

lying in the plane ρ, parallel to the growth direction. The thickness ratio of thick and thin Jahn–Teller domains (d_1/d_2) changes along the crystal due to different stress conditions originating from the preparation. By annealing the specimen in a protective atmosphere (to avoid oxidation) at 230°C, which is above the tetragonal–cubic transition temperature (200°C), some small changes in the configuration of these elastic domains were observed, but the overall configuration remains very similar. Moreover, no X-ray line broadening was observed in the X-ray powder data of the annealed sample, which implies that no Mn^{3+} clustering or inhomogeneities in the sample are induced by this annealing [4].

On sample No. 2 the Jahn–Teller domains were only observed on a part of the cube, plane ρ, at a longer distance from the seed crystal in the form of very vague stripes together with the growth striations (Fig. 2). In this case the thicknesses of the Jahn–Teller domains were less than or comparable with the space resolution of the method.

Sample No. 1 was additionally used for reciprocal space mapping. An 18 kW rotating anode X-ray generator and BEDE-SCIENTIFIC triple-crystal diffractometer were used in the (Si 2 2 0, –$Mn_2Fe_3O_{12}$ 4 0 0) setting. A thin slit in front of the detector was used as an analyser. The obtained part of reciprocal space is shown in Fig. 3. The map consists of two spots. The bigger one in [0, 0] position corresponds to the thicker domains (the irradiated area consists of circa 5 domains of one grain only), which have the tetragonal deformation in the [0 0 1] direction, perpendicular to the surface plane ρ. The sharp intense peak is surrounded by a large area of strong diffuse scattering, which indicates the presence of many defects in the sample.

The weak spot corresponds to thin domains which have the tetragonal deformation along the [1 0 0] direction, parallel to the growth direction. The diffraction signal is three orders less than the main peak. The elongated shape of this spot which is directed towards the main one and the indication of the ridge connecting the two spots shows, that the tetragonal deformation is not homogeneous in the thin domains. This measurement cannot give the absolute value of the lattice constants, but if we take for the parameter c_1 (i.e. the position of the main spot) the value $c = 8.8$ Å for the thick domains, we find, that the parameter a in the thin domains of the measured sample is in the range from 8.2 to 8.4 Å.

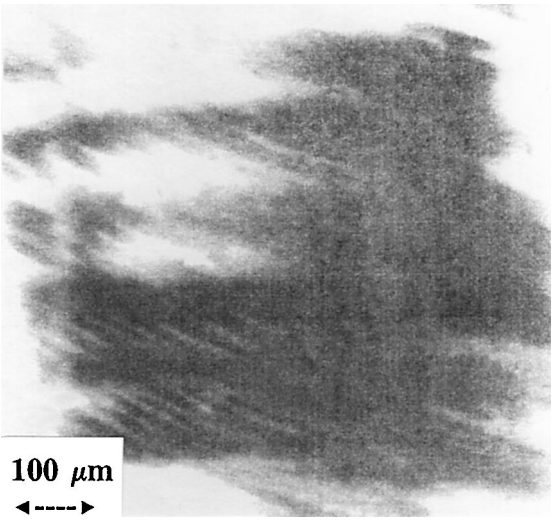

Fig. 2. Double-crystal topography of a part of sample No. 2. The thick patterns are the growth striations, the thin ones are the images of the Jahn–Teller domains.

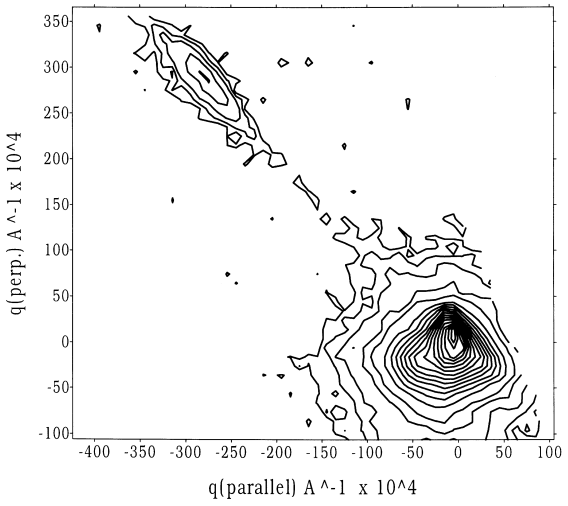

Fig. 3. The reciprocal space map around the (0 0 4) reflection.

4. Composition and the surface structure

The formation of the Jahn–Teller domains means that the surface parallel to the ρ plane has the form of a saw-tooth roof. This relief is not completely suppressed by polishing, so that on sample No. 2 the set of darker and brighter 'domains' is seen both by optical microscopy and by SEM (secondary electron mode — Figs. 4a and b). The width of these 'domains', d_1 and d_2 and their ratio change at a large range along the growth direction due to the variable growth conditions. In the case of Fig. 4b the thickness of these 'domains' is likely to correspond to dimensions of Jahn–Teller domains imaged by X-ray topograph (Fig. 2).

Electron probe microanalysis performed in many points of darker and brighter 'domains' gave the same results (corresponding to the formula Mn_2FeO_4) within the accuracy of this method.

5. Magnetic domains

The magnetic domain structure was imaged using the colloid-SEM method (i.e. observing the dried Bitter patterns in a scanning electron microscope [3]) on two different planes ρ and σ of sample No. 2. The sample was demagnetised by a decreasing AC field, after which a drop of ferrofluid was dried in zero magnetic field on the surface of the sample.

Typical examples of the magnetic domain structure on the plane ρ are illustrated in Figs. 5a and b. Parallel areas (stripes) without visible magnetic domain structure and stripes with irregular dense magnetic domain patterns alternate. These patterns reflect the surface magnetic domains which partly compensate the stray fields of the inner magnetic domains that have a large magnetisation component perpendicular to the surface. The very large density of the colloidal particles on the domain walls show that the compensation of the stray fields is incomplete, i.e. magnetic charges are on the surface [6]. In the areas without a visible magnetic domain structure the magnetisation is parallel to the surface. We suppose the existence of 180° walls that separate antiparallel magnetic domains. They are not visible due to the fact that their stray fields and their gradients are substantially weaker in comparison with the changes of the stray fields of the surface magnetic domains of neighbouring uncompensated stripes, so that they do not attract the colloidal particles.

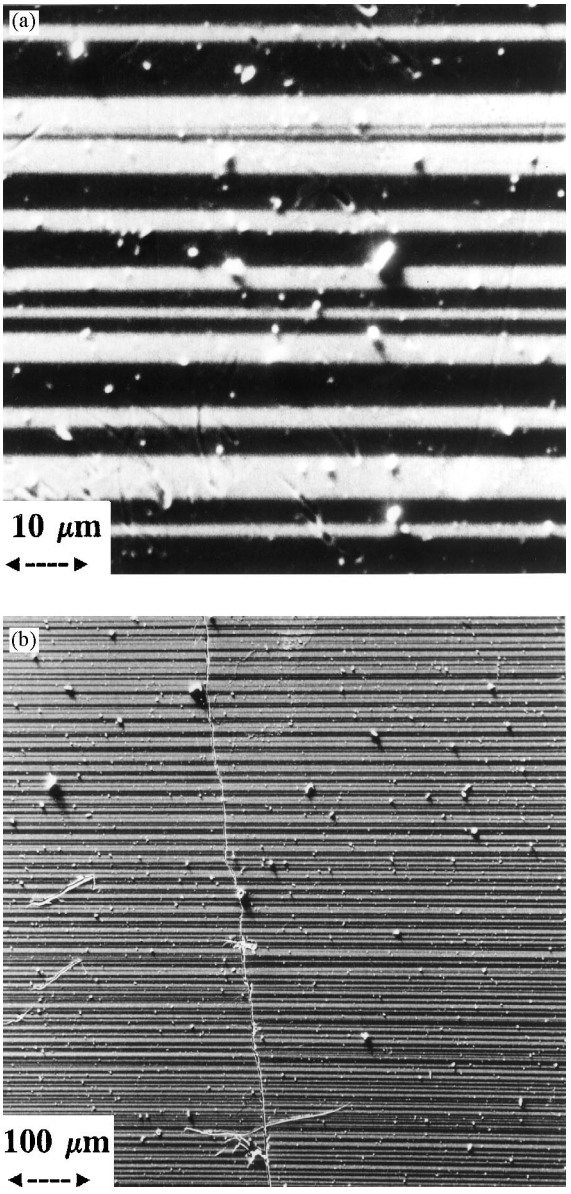

Fig. 4. The darker and brighter 'domains' with different d_1 and d_2 thicknesses at a shorter distance (Fig. 4a) and larger distance (Fig. 4b) from the seed crystal, respectively (ρ plane of sample No. 2) are imaged using the secondary electron mode (SEM).

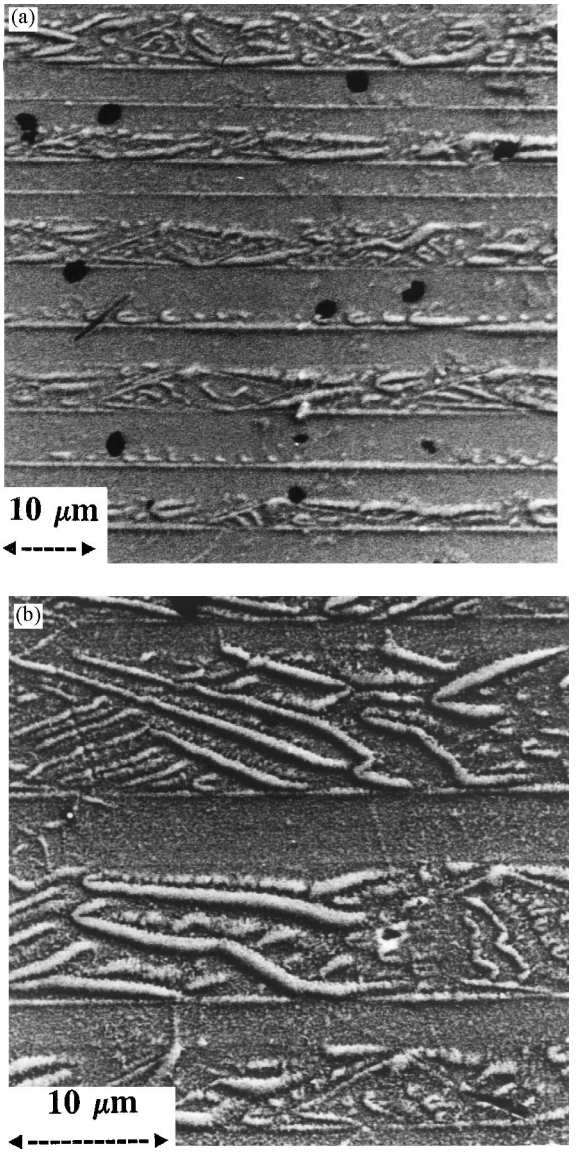

Fig. 5. (a) and (b) The typical magnetic domain structure on the plane ρ of sample No. 2 (after in-plane AC demagnetisation) in zero external magnetic field. The stripes are perpendicular to the growth direction.

The magnetic domain structure observed on the σ plane is different from the magnetic domain structures on the plane ρ and shows only stripes with closure domains (Figs. 6a and b). The direction of these stripes makes an angle of 45° with respect to the planes ρ and ω which means parallel to the Jahn–Teller domains coinciding with the crystallographic orientation of the (1 1 0) plane. The broad stripes with a complicated surface structure of closure magnetic domains are seen on the major part of the surface of the σ plane. Only on a small part of the surface, narrow stripes as shown in Fig. 6c are observed. From the visualised magnetic domain structure we may conclude that the magnetisation is perpendicular and/or has a substantial component perpendicular to the σ plane. In fact, no domains with a magnetisation parallel to the surface could be observed after demagnetisation, independent of the chosen magnetic field direction during the demagnetisation.

6. VSM results

For a better understanding of the complex magnetic domain structure, VSM hysteresis loop measurements were performed in the directions perpendicular to the three planes ρ, σ and ω (see Figs. 7a–c).

In loops taken in the fields perpendicular to ρ and ω (Figs. 7a and c) two distinct parts can be distinguished: the central steep part at low field, corresponding to the magnetisation process by wall motion in those parts of the sample where the easy axes are parallel to the field direction, and the outer parts, indicating magnetisation by rotation in regions with easy axes perpendicular to the field direction. Such rotation processes are not observed when the field is perpendicular to the σ plane (Fig. 7b) which indicates that the easy axes are perpendicular to the σ plane in the whole sample, in accordance with the domain patterns observed on this plane (Figs. 6a and b).

The results of the X-ray topography experiments indicate that the crystallographic c-axis of the elastic domains are perpendicular to either the ω or ρ plane, but not to the σ plane, which implies that the crystallographic c-direction is not an easy axis of magnetisation. From the large negative magnetostriction $\lambda_{1\,0\,0}$ in the cubic part of the $Mn_xFe_{3-x}O_4$ system [7] and the tetragonal structure of Mn_2FeO_4 with $c/a > 1$, the magnetoelastic energy favours also an easy magnetisation axis perpendicular to the c-axis. Conversely, a theoretical

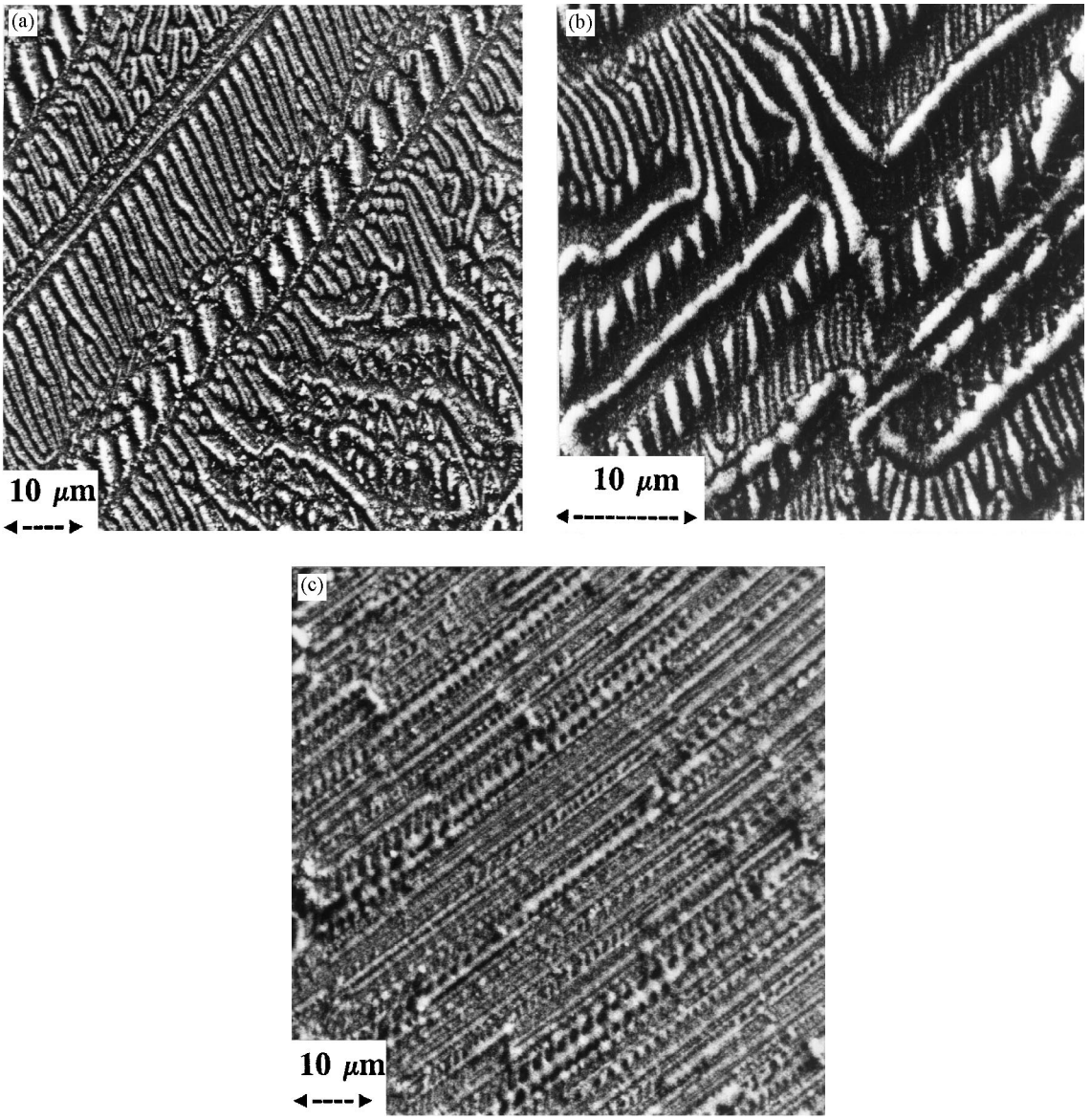

Fig. 6. (a) and (b) The magnetic domain structure of closure domains on the plane σ of sample No. 2 (after AC demagnetisation perpendicular to the plane) in zero external magnetic field. (c) The parallel narrow stripes make an angle of 45° with respect to the plane ρ and ω (i.e. coinciding with the Jahn–Teller domains crystallographic orientation).

analysis of the single ion magnetocrystalline anisotropy for Mn^{3+} ions leads to an easy c-axis [8]. However, in Mn-ferrites the spin arrangements are believed to be non-collinear, which strongly influences the anisotropy energy and can also lead to an easy plane of magnetisation for large spin-canting angles. Neutron diffraction experiments on magnetically aligned powder samples indeed showed that the easy axis of magnetisation does not coincide with the c-axis and a non-collinear magnetic structure occurs [9,10]. Unfortunately, these experiments were performed on slowly cooled

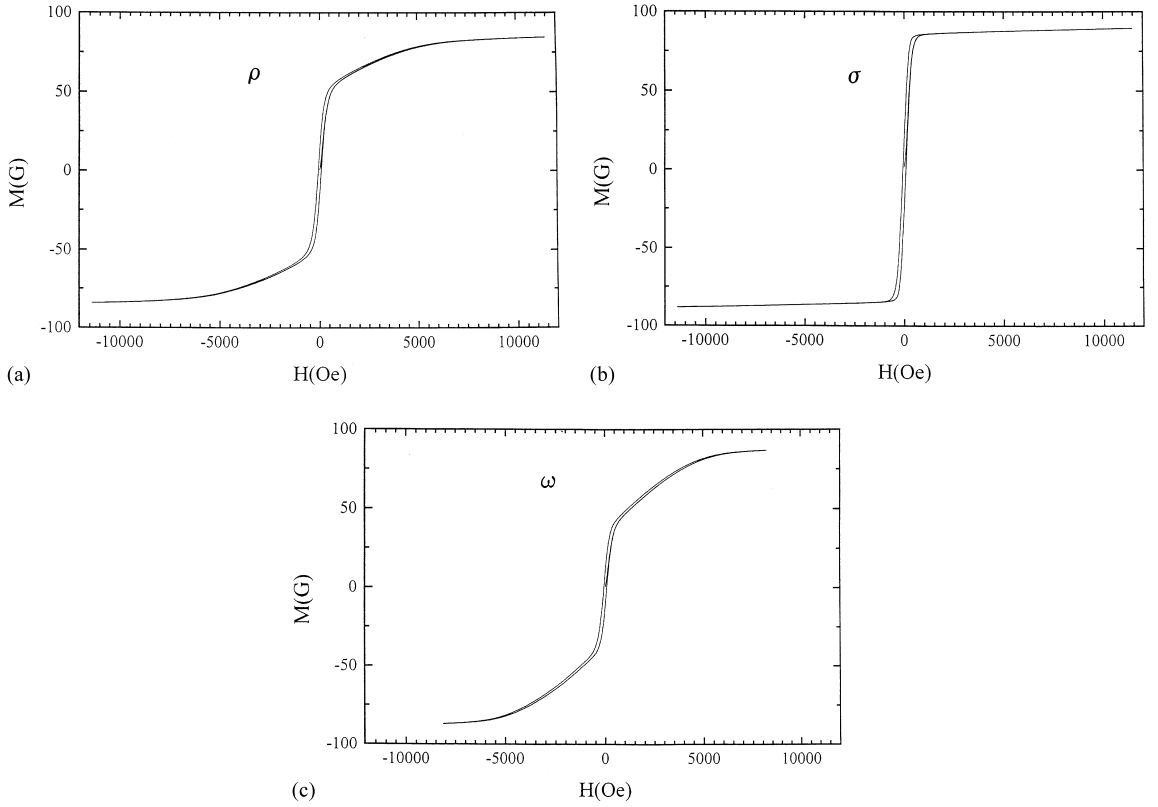

Fig. 7. (a–c) The VSM loops taken in the magnetic fields perpendicular to ρ, σ or ω, respectively.

specimens, which raises some questions on the chemical homogeneity of these samples [11]. From the experimental VSM curves an approximate value of the saturation magnetisation, $M_s = 85\,\mathrm{G}$ and of the anisotropy constant $K = 2 \times 10^5\,\mathrm{erg/cm^3}$ were determined. The dominance of anisotropy energy over the demagnetising energy is in agreement with the open domain structures with free magnetic poles, observed in the domain patterns.

7. Conclusions

Jahn–Teller domains of the bulk Mn_2FeO_4 are present as alternating thick/thin domains separated by (1 1 0) planes. The c_1 tetragonal axis of thick Jahn–Teller domains is oriented perpendicularly to the growth direction, whereas the c_2 tetragonal axis in thin Jahn–Teller domains is oriented along the growth direction.

The crystal lattice parameters of the powdered sample are $c = 8.8521\,\text{Å}$, and $a = 8.3722\,\text{Å}$ with a positive c/a value: 1.0573. However, a variation of the tetragonal c/a value occurs in the thin Jahn–Teller domains, which might be correlated to lattice relaxation but not to chemical inhomogeneities of the bulk sample.

The magnetic domain structure on the ρ plane consists of two kinds of magnetic domain structures, which can be related to the orientation of the c-axis perpendicular and parallel to the surface, respectively. The dominant orientation of the magnetic domain structure on the σ plane coincides with the orientation of the (1 1 0) Jahn–Teller domains.

The observations of magnetic domain structures on the ρ and σ planes are not mutually consistent. On the σ plane the magnetisation is perpendicular to the surface and on a part of the ρ plane the magnetisation is also perpendicular to the surface and/or has a large component perpendicular to the surface.

The VSM measurements are also difficult to be correlated with the domain observations. This leads us to the assumption that the domain structure observed on the surfaces does not necessarily correspond entirely to the internal domain structure.

Evaluating the observation of the Jahn–Teller domains, magnetic domains and magnetisation loops, we conclude that there exist

- an easy axis perpendicular to the plane σ
- easy axes perpendicular to the plane ρ and ω (i.e. perpendicular to the tetragonal c_1-and c_2-axes), which means that the tetragonal c-axis might be a hard direction of magnetisation.

Acknowledgements

Thanks are due to J. Kadlecová and L. Půst for performing the VSM measurements.

References

[1] J. van Landuyt, R. de Ridder, V.A.M. Brabers, S. Amelinckx, Mater. Res. Bull. 7 (1972) 327.
[2] W. Graff, J. Kub, K. Wieteska, Phys. Stat. Sol. A 126 (1991) 477.
[3] J. Šimšová, R. Gemperle, J.C. Lodder, J. Magn. Magn. Mater. 95 (1991) 85.
[4] V.A.M. Brabers, J. Phys. Chem. Sol. 32 (1971) 2181.
[5] V.A.M. Brabers, J. Crystal Growth 8 (1971) 26.
[6] J. Kaczér, R. Gemperle, Czech. J. Phys. B 10 (1960) 505.
[7] V.A.M. Brabers, J. Appl. Phys. 42 (1971) 4525.
[8] P. Novák, Czech. J. Phys. B 16 (1966) 723.
[9] B. Boucher, R. Buhl, M. Perrin, J. Phys. Coll. 32 (1971) C1-322.
[10] B. Boucher, R. Buhl, M. Perrin, J. Appl. Phys. 40 (1970) 1126.
[11] R. Buhl, J. Phys. Chem. Sol. 30 (1969) 805.